

POISEUILLE FLOW OF AN ARRHENIUSLY REACTIVE POWER LAW FLUID INCORPORATED WITHIN PARALLEL PLATES USING REGULAR PERTURBATION METHOD AND DIRECT INTEGRATION

*Ibrahim Aliyu, Ishaq Zainab A. and Ishaq Maimuna A.

Department of General Studies, Minna Institute of Technology and Innovation, Minna, Niger State

*Corresponding Author Email Address: aliyuibrahim076@gmail.com

ABSTRACT

This paper presents an approximate analytical solution capable of analyzing the velocity, temperature and concentration distribution in the poiseuille flow of an arrheniusly reactive power law fluid incorporated within parallel plates. The equations governing the phenomenon are solved analytically using regular perturbation method and direct integration, to show the influence of the parameter involved on the system. The effect of change in parameters such as the power law index, the pressure gradient coefficient, the viscous heating parameter, the Arrhenius chemical reaction rate and the Frank-Kamenetskii number are presented graphically and discussed. The result obtained revealed that the power law index, the pressure gradient coefficient, the viscous heating parameter, the Frank-Kamenetskii number and the Arrhenius chemical reaction rate enhanced the fluid flow, average temperature and species concentration.

Keywords: Arrheniusly reactive, Parallel plates, Poiseuille flow, Power law fluid, Regular perturbation method.

INTRODUCTION

Non-Newtonian fluids refers to a specific category of fluid which exhibits variable viscosity under the action of force. It certainly differs from the Newtonian fluid which follows Newton's law of viscosity and bears constant viscosity under stress. The physical viscosity in non-Newtonian fluids could be dependent on the magnitude of the shear stress (e.g., shear-thickening/dilatants fluids, shear-thinning/pseudoplastic fluids, Bingham plastics, etc.) (Kavitha, 2020).

Many fluids used in industrial and engineering processes like geological materials, liquid foams, polymeric fluids hydrocarbon oils and grease do exhibit flow characteristics that cannot be adequately described by the classical linearly viscous model (Makinde, 2009).

Non-Newtonian flows are often encountered in both science and technology applications such as oil recovering, soil remediation or biological engineering, where the solution with polymeric additive, mud, blood, colloids exhibits non-Newtonian features (Siddiqui *et al.*, 2013). Reactive flows are flows in which there are interactions between chemical reactions and fluid dynamics (Siddiqui *et al.*, 2013).

A non-Newtonian fluid is a fluid that does not follow Newton's law of viscosity that is, constant viscosity independent of stress. In non-Newtonian fluids, viscosity can change when under force to either more liquid or more solid. Many salt solutions and molten polymers are non-Newtonian fluids, as are many commonly found

substances such as custard, honey toothpaste, starch suspension, paint, blood and shampoo (Ouellette, 2013).

The study of heat transfer and thermal stability of reactive non-Newtonian fluid is extremely important for the safety of life and proper handling of materials during processing (Haroon *et al.*, 2011).

In industrial applications, most of the fluids have non-Newtonian fluids characteristics. It is of great significance to the economic development and energy consumption. The use of liquids in various technical applications is well known, but there is greater special interest of researchers in the study of non-Newtonian fluids because of the realization that they are now very common in everyday life (farayola, 2017).

A pair of scissor is an example to demonstrate shear forces when a piece of paper placed between the two metal blades of a pair of scissors, it gets divided into two parts only because of the shear force.

In chewing food, the force applied by the teeth on the food acts in a perpendicular direction. This helps the food to get divided into smaller units or sections after every chew. The repeated chew or application of shear force makes the food particles small and swallowing process easy.

In view of the above, this paper aim at establishing approximate analytical solution capable of analyzing velocity, temperature and concentration distribution in the poiseuille flow of an arrheniusly reactive power law fluid between parallel plates incorporating species of concentration equation.

Haroon *et al.* (2011) considered the steady flow of a reactive power law fluid with the generation of heat due to a chemical reaction under Arrhenius kinetics, confined between two infinitely long plates. They examined the properties of the solutions and solved the model equation analytically using direct integration and Homotopy perturbation methods. Their model equations are:

. *Momentum equation*

$$\frac{d}{dy} \left(\frac{du}{dy} \right)^{2m+1} = C \quad (1)$$

Energy equation

$$\frac{d^2\theta}{dy^2} + \Gamma \left(\frac{du}{dy} \right)^{2m+2} + \mathcal{F}(\theta; \beta, n) = 0 \quad (2)$$

From the findings of his work, he conclude that the behavior of the fluid depends not only on the power law, but also on the pressure gradient and the gap between the parallel plates. The magnitude of velocity between the parallel plates for shear thinning case is very large as compared to the viscous and shear thickening cases. The velocity increases with the increases in pressure gradient for all values of the power law index, m . Temperature increases with the increase of viscous heating parameter. For shear thinning fluid the temperature distribution decreases with an increase in the Frank-Kamenetskii parameter, δ , but for viscous and shear thickening cases, the temperature increases with an increase in Frank-Kamenetskii parameter, δ . There is prominent change in temperature profile for any type of chemical reaction for small values of δ . But with the increase in δ , we observe that the temperature decreases with an increase in n . When the activation energy $\beta \ll 1$ there is no change in the temperature profile for any type of chemical reactions.

Siddiqui *et al.* (2013) considered a steady state, unidirectional and incompressible flow of a power law of a reacting fluid in the z -direction inside a pipe of a uniform cross-section with isothermal wall at $r = a$. They examined the properties of the solution and solved the model equations analytically via direct integration and homotopy perturbation methods. Their model equations are:

Momentum equation

$$\frac{1}{r} \left(\frac{d}{dr} \left(r \frac{dw}{dr} \right) \right)^{2m+2} = C$$

(3)

Energy equation

$$\frac{1}{r} \frac{d}{dr} \left(r \frac{d\theta}{dr} \right) + \Gamma \left(\frac{dw}{dr} \right)^{2m+2} + \mathcal{F}(\theta, \beta, n) = 0$$

(4)

From the findings of this work, we conclude that in Poiseuille flow the behavior of the fluid depends not only on the power law index, m , but also on the pressure gradient and the gap between the walls. We also find that the magnitude of velocity between the walls for shear thinning case is very large as compared to the viscous and shear thickening cases, that is, the magnitude of velocity decreases with the increases in m . Chemical reaction terms play an important role to change temperature distribution in the pipe. The temperature increases with the increases in viscous heating parameter, Γ . The temperature increases for shear thinning fluid is compared to the viscous and shear thickening cases. When the activation energy, $\beta \ll 1$, we do not observe any change in the temperature profile cases. With the increase in β , the temperature increase near the walls and decreases at the center for the shear thinning cases.

Farayola. (2017) considered a steady flow of a reactive viscous fluid in a porous cylindrical pipe with isothermal wall under Arrhenius kinetics with inclusion of porosity force (permeability) in the momentum equation. A regular perturbation technique was employed to obtain an approximate solution of the resulting dimensionless non-linear equations. Their model equations are:

$$\frac{1}{r} \frac{d}{dr} \left(r \frac{d\theta}{dr} \right) + \lambda e^\theta + \alpha \beta e^{-\theta} \left(\frac{du}{dr} \right)^2 = 0$$

$$\frac{1}{r} \frac{d}{dr} \left(r e^{-\theta} \frac{du}{dr} \right) + \delta e^{-\theta} u = -1$$

(5)

(6)

From his findings, he conclude that the viscous heating parameter has effect on the temperature and velocity profiles of the flow. The presence of pores on the geometry of the problem also has effect on the temperature and velocity of the fluid. Increase in the permeability parameter increases the velocity of the fluid. The temperature is also enhanced than when there is no porosity. From the work, it could be said that the temperature of the fluid can be controlled by varying the viscous heating parameter and thermal conductivity in order to minimize their effects and maximize the flow system efficiency.

MATERIALS AND METHODS

Model Formulation

Here, the work of Haroon *et al.* (2011) is extended by incorporating species of concentration equation. The respective conservation equations governing the phenomena are:

Equation of momentum:

$$2^m \eta (2m + 1) \left(\frac{du}{dy} \right)^{2m} \left(\frac{d^2u}{dy^2} \right) = \frac{dp}{dx} \quad (1)$$

Equation of energy

$$K(T) \frac{d^2T}{dy^2} + 2^m \eta \left(\frac{du}{dy} \right)^{2m+2} + QCJ \left(\frac{kT}{vh} \right)^n e^{-\frac{E}{RT}} = 0$$

(2)

Equation of species concentration:

$$D(T) \frac{d^2C}{dy^2} - CJ \left(\frac{kT}{vh} \right)^n e^{-\frac{E}{RT}} = 0 \quad (3)$$

The boundary conditions for this geometry are:

$$\left. \begin{aligned} \frac{du}{dy} \Big|_{y=0} &= 0, u(y_0) = 0 \\ \frac{dT}{dy} \Big|_{y=0} &= 0, T(y_0) = T_0 \\ \frac{dC}{dy} \Big|_{y=0} &= 0, C(y_0) = C_0 \end{aligned} \right\} \quad (4)$$

Where

$$K(T) = K_0 \left(\frac{T}{T_0} \right) \quad (5)$$

$$D(T) = D_0 \left(\frac{T}{T_0} \right) \quad (6)$$

Where

C is concentration of reactant species, E is the activation energy, f is the vibration frequency, h is the Planck's number, J is the rate constant, k is the Boltzmann's constant, K is the thermal conductivity of the material, m is the flow behavior index, n is a numerical exponent, Q is the heat reaction, R is the universal gas content, T is the temperature, T_0 is the wall temperature, η is the apparent viscosity

Method of Solution

Non-dimensionalisation

Here, equations (1) --- (4) were non-dimensionalized using the following set of dimensionless variable:

$$u^1 = \frac{u}{U}, \quad y^1 = \frac{y}{y_0}, \quad \phi = \frac{C}{C_0}, \quad \theta = \frac{E}{RT_0} (T - T_0) \quad (7)$$

Using (7) in (1) – (6), and after dropping the prime, equation (1) – (4) become

$$\frac{d}{dy} \left(\frac{du}{dy} \right)^{2m+1} = \beta \quad (8)$$

$$K_0(1 + \varepsilon\theta) \frac{d^2\theta}{dy^2} + \gamma \left(\frac{du}{dy} \right)^{2m+2} + \delta\phi(1 + \varepsilon\theta)^n e^{\frac{\theta}{1+\varepsilon\theta}} = 0 \quad (9)$$

$$D_0(1 + \varepsilon\theta) \frac{d^2\phi}{dy^2} - \alpha(1 + \varepsilon\theta)^n \phi e^{\frac{\theta}{1+\varepsilon\theta}} = 0 \quad (10)$$

$$\left. \begin{aligned} \frac{du}{dy} = 0, u(1) = 0 \\ \frac{d\theta}{dy} = 0, \theta(1) = 0 \\ \frac{d\phi}{dy} = 0, \phi(1) = 1 \end{aligned} \right\} \quad (11)$$

Where

$$\beta = \frac{y_0}{2^m \eta} \left(\frac{y_0}{U} \right)^{2m+1} \frac{dp}{dx}, \quad \beta \text{ is the pressure gradient coefficient parameter and } U \text{ is the reference velocity}$$

$$\gamma = 2^m \eta \frac{y_0^2}{\varepsilon T_0} \left(\frac{U}{y_0} \right)^{2m+2}, \quad \gamma \text{ is the viscous heating parameter.}$$

$$\delta = \frac{QJC_0 k^n T_0^n y_0^2}{v^n h^n \varepsilon T_0} e^{-\frac{E}{RT_0}}, \quad \delta \text{ is the Frank-Kamenetskii number and } C_0 \text{ is the initial concentration of reactant.}$$

$$\alpha = \frac{Jk^n T_0^n y_0^2 e^{-\frac{E}{RT_0}}}{v^n h^n}, \quad \alpha \text{ is the Arrhenius chemical reaction rate}$$

3.2.2 Analytical Solution

Using regular perturbation method and direct integration, the approximate analytical solution of equation (8) – (11) is obtained as:

$$u(y) = \frac{2m+2}{2m+1} \beta^{\frac{1}{2m+1}} \left(1 - y^{\frac{2m+2}{2m+1}} \right) \quad (12)$$

$$\phi(y) = N \cos py + \varepsilon (c_1 \cos py + \sigma \cos^2 py + \sigma_1 \sin^2 py + \sigma_2 \gamma_1 y^s \cos py) \quad (13)$$

$$\theta(y) = A \cos py + B y^g + C + \varepsilon \left\{ \begin{aligned} & \left(2 \frac{\delta}{K_0} p((n+a)AN + \sigma - \sigma_1) - 2A^2 P^3 \right) P(\cos^2 py - \sin^2 py) \\ & - ABg(g-1)(g-2)(g-3)y^{g-4} \cos py + \\ & ABpg(g-1)(g-2)y^{g-3} \sin py \\ & - ABpg(g-1)(g-2)y^{g-3} \sin py - ABp^2 g(g-1)y^{g-2} \cos py \\ & + \left[-\frac{\delta}{K_0} ((n+a)BNg + \sigma_2 \gamma_1 g) + ABp^2 g \right] (g-1)y^{g-2} \cos py \\ & - \left[-\frac{\delta}{K_0} g((n+a)BN + \sigma_2 \gamma_1) + ABp^2 g \right] py^{g-1} \sin py \\ & + \left[-ABp^3 + \frac{\delta}{K_0} p(\sigma_2 \gamma_1 + (n+a)BN) \right] gy^{g-1} \sin py \\ & + \left[-ABp^3 + \frac{\delta}{K_0} p(\sigma_2 \gamma_1 + (n+a)BN) \right] py^g \cos py - \\ & \left. \left[2B^2 g(g-1)^2 (2g-3)y^{2(g-2)} + \frac{\delta}{K_0} p((n+a)CN + c_1) - ACp^3 \right] p \cos py + \right. \\ & \left. BCg(g-1)(g-2)(g-3)y^{g-4} + C_4 \right\} \end{aligned} \right.$$

(14)

Where

$$N = \frac{1}{\cos p}$$

$$p = \sqrt{\frac{\alpha_0}{D_0}}$$

$$c_1 = -\frac{\sigma \cos^2 p + \sigma_1 \sin^2 p + \sigma_2 \gamma_1 \cos p}{\cos p}$$

$$\sigma = \frac{\left(\frac{2p^2 - \frac{\alpha_0}{D_0}}{2p^2} \right) AN \left(p^2 - \frac{\alpha_0(n+a)}{D_0} \right)}{2p^2 \left(1 - \frac{\left(2p^2 - \frac{\alpha_0}{D_0} \right)}{2p^2} \right) + \frac{\alpha_0}{D_0} \left(\frac{2p^2 - \frac{\alpha_0}{D_0}}{2p^2} \right)}$$

$$\sigma_1 = \frac{AN \left(p^2 - \frac{\alpha_0(n+a)}{D_0} \right)}{2p^2 \left(1 - \frac{\left(2p^2 - \frac{\alpha_0}{D_0} \right)}{2p^2} \right) + \frac{\alpha_0}{D_0} \left(\frac{2p^2}{2p^2} \right)}$$

$$\sigma_2 = - \frac{BN \left(p^2 - \frac{\alpha_0(n+a)}{D_0} \right)}{\gamma_1 \left(p^2 - \frac{\alpha_0}{D_0} \right)}$$

$$C_4 = \left(2 \frac{\delta}{K_0} p((n+a)AN + \sigma - \sigma_1) - 2A^2 p^3 \right) p(\cos^2 p - \sin^2 p)$$

$$- ABg(g-1)(g-2)(g-3)\cos p + ABpg(g-1)(g-2)\sin p$$

$$- ABpg(g-1)(g-2)\sin p - ABp^2g(g-1)\cos p$$

$$+ \left(- \frac{\delta}{K_0} ((n+a)BNg + \sigma_2\gamma_1g) + ABp^2g \right) (g-1)\cos p$$

$$- \left(- \frac{\delta}{K_0} g((n+a)BN + \sigma_2\gamma_1) + ABp^2g \right) p \sin p + \left(- ABp^3 + \frac{\delta}{K_0} p(\sigma_2\gamma_1 + (n+a)BN) \right) g \sin p$$

$$+ \left(- ABp^3 + \frac{\delta}{K_0} p(\sigma_2\gamma_1 + (n+a)BN) \right) p \cos p - 2B^2g(g-1)^2(2g-3) +$$

$$\left(\frac{\delta}{K_0} p((n+a)CN + C_1) - ACp^3 \right) p \cos p + BCg(g-1)(g-2)(g-3)$$

The computation are done using computer symbolic algebraic package MAPLE 17.

RESULTS AND DISCUSSION

To conclude this analysis we examine the relationship between the power law index (m), the pressure gradient coefficient (β), the viscous heating parameter (γ), the Frank-Kamenetskii number, (δ) and the chemical reaction rate (α). Analytical solution given by equation (12) – (14) is computed using computer symbolic algebraic package MAPLE 17. The numerical results obtain from the method are shown in figure 1 to 5.

Figure 1. depicts the graph of velocity $u(y)$ against distance y for different values of power law index, m . It is observed that the velocity decreases with distance and increases as the power law index increases.

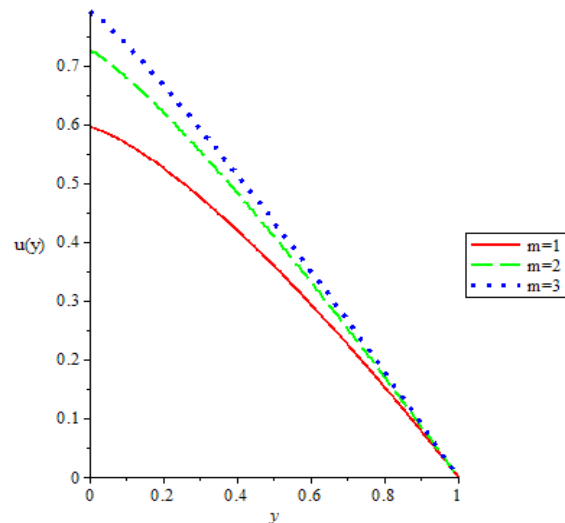


Figure 1: Graph of velocity $u(y)$ against distance, y for different values of power law index when $\delta = 0.5, \gamma = 1, D_0 = 1, \alpha = 0.2, K_0 = 0.4, \varepsilon = 0.01, n = 0, \beta = 0.5$

Figure 2 depicts the graph of velocity $u(y)$ against distance y for different values of pressure gradient coefficient β . It is observed that the velocity decreases along the distance but increases with increase in pressure gradient coefficient.

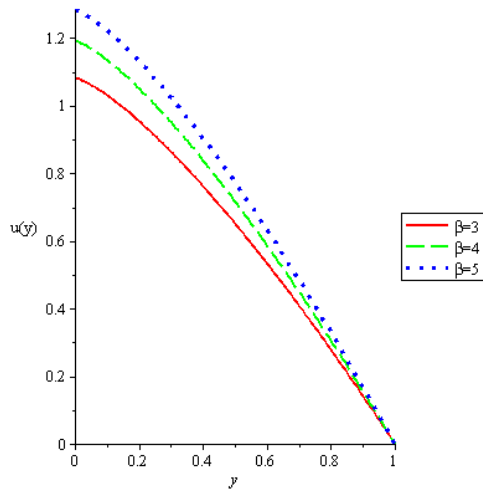


Figure 2.: Graph of velocity $u(y)$ against distance y for different values of pressure gradient coefficient β when $\delta = 0.5, \gamma = 1, D_0 = 1, \alpha = 0.2, K_0 = 0.4, \varepsilon = 0.01, n = 0, m = 1$

Figure 3 depicts the graph of temperature $\theta(y)$ against distance y for different values of viscous heating parameter γ . It is observed that the temperature increases and later decreases with distance and increases as viscous heating parameter increases.

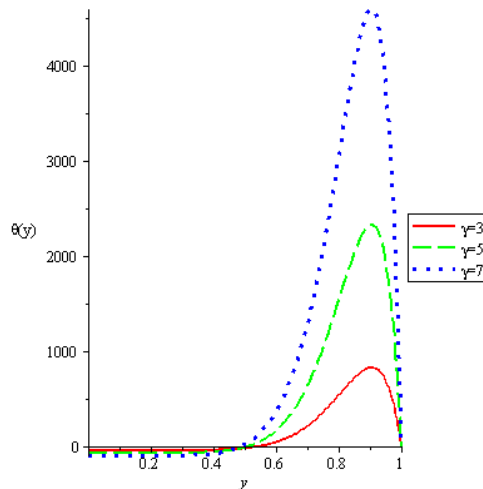


Figure 3: Graph of temperature $\theta(y)$ against distance y for different values of viscous heating parameter γ when $\delta = 0, m = 0, \beta = 4, D_0 = 1, \alpha = 0.1, K_0 = 0.1, \varepsilon = 0.01, n = 0.5$

Figure 4 shows the graph of temperature $\theta(y)$ against distance y for different values of Frank-Kamenetskii number δ . It is observed that the temperature decreases along the distance and maximum temperature increases as Frank-Kamenetskii number increases.

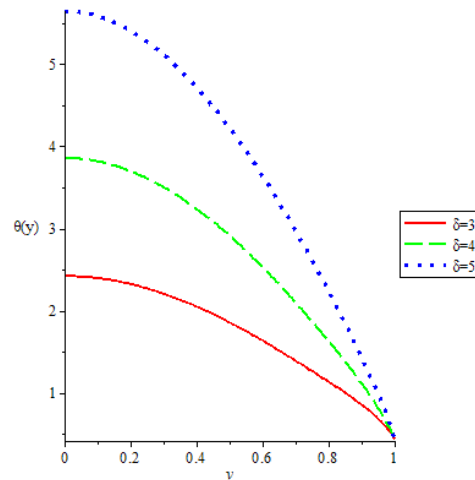


Figure 4: Graph of temperature $\theta(y)$ against distance y for different values of Frank Kamenetskii number δ when $m = 0, \beta = 4, \gamma = 1, D_0 = 1, K_0 = 0.1, \alpha = 0.1, n = 0, \varepsilon = 0.01$

Figure 5 depicts the graph of concentration $\phi(y)$ against distance y for different values of Arrhenius chemical reaction rate α . It is observed that the concentration decreases along the distance and increases as Arrhenius chemical reaction rate increases.

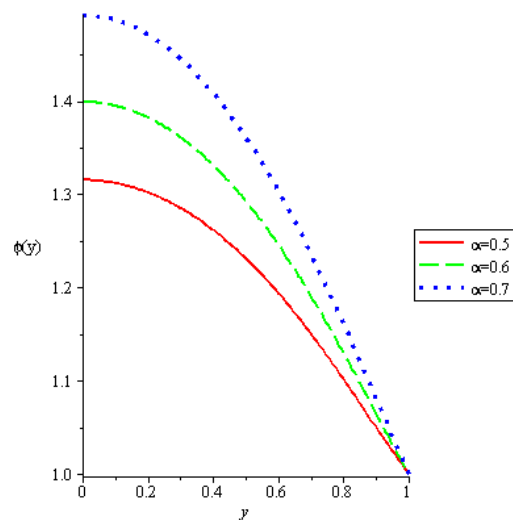


Figure 5: Graph of concentration profile $\phi(y)$ against distance y for different values of Arrhenius chemical reaction rate α when $n = 0.5$

$$\delta = 0, \beta = 4, m = 0, D_0 = 1, K_0 = 0.4, \gamma = 1, \varepsilon = 0.01, n = 0$$

Conclusion

For a high activation situation that is, as $\varepsilon \rightarrow 0$, we have solved the equations governing the poiseuille flow of an arrheniusly reactive power law fluid between parallel plates incorporating species of concentration equation analytically using regular perturbation method and direct integration. From the result obtained we can conclude that:

1. Power law index and Pressure gradient coefficient enhanced fluid flow.
2. Viscous heating parameter and Frank-Kamenetskii number enhanced average temperature.
3. Arrhenius chemical reaction rate enhanced species concentration.

The results obtained are not only expected to guide manufacturers but also to assist other researchers to better understand poiseuille flow of an arrheniusly reactive power law fluid between parallel plates.

REFERENCES

- Farayola, P. I. (2017). On Steady Flow of a Reactive Viscous Fluid in a Porous Cylindrical pipe. *Open Journal of Fluid Dynamics*, 7, 359-370. Retrieved from: <https://doi.org/10.4236/ojfd.2017.73024>.
- Haroon, T., Ansari, A. R. Siddiqui, A. M. and Jan, S. U. (2011). Analysis of Poiseuille Flow of a Reactive Power Law Fluid Between Parallel Plates. *Applied Mathematical science*, Vol. 5 no. 55. 2721 – 2746
- Kavitha, P (2020). Computational Methods For Non-Newtonian Power Law Fluids. *Journal of Critical Reviews* Vol.7. DOI: <http://dx.doi.org/10.31838/jcr.07.13.04>
- Kerehalli, V. P, Seetharam, R. S. and Pampana, S (2012). Non-Newtonian Power Law Fluid Flow and Heat Transfer over a Non-Linearly Stretching Surface. Vol. 3 No.5 (2012). Retrieved from <https://www.Scrip.org>. DOI: 10.4236/am.2012.35065.
- Makinde. O. D. (2009). Thermal Criticality for a Reactive Gravity Driven Thin Film Flow of a Third- Grade Fluid with Adiabatic Free Surface down an Inclined Plane. *Applied Mathematics and Mechanics*, 30, 373 – 380. Retrieved from: <https://doi.org/10.1007/s10483-009-0311-6>.
- Siddiqui, A. M., Haroon, T., Jan, S. U. and Babcock, B. S. (2013). Steady Flow of Reactive Power Law Fluid in a Cylindrical Pipe with an Isothermal Wall. *Applied Mathematical Sciences*, Vol. 7, 2013, no. 141, 7037 – 7051. Retrieved from: www.m-hikari.com or <https://dx.doi.org/10.12988/ams.2013.36316>.
- Springer, B. H. (2008). Introduction, Importance and Development of Fluid Mechanics pp: 1–14. Retrieved from <https://link.springer.com/doi.org/10.1007/978-3-540-71343-2-1>.
- Taha, A. and Mohammed, F. M. (2017). Application of Group Theoretical Methods to non-Newtonian Fluids Flow Models. *Mathematical Problems in Engineering*, Vol. 2017, Article ID. Retrieved From: <https://doi.org/10.1155/2017/6847647>.